Title
Switchable assembly and function of antibody complexes in vivo using a small molecule

Journal
Proceedings of the National Academy of Sciences of the United States of America, 119(9)

ISSN
0027-8424

Authors
Martinko, Alexander J
Simonds, Erin F
Prasad, Suchitra
et al.

Publication Date
2022-03-01

DOI
10.1073/pnas.2117402119

Peer reviewed

Switchable assembly and function of antibody complexes in vivo using a small molecule

Alexander J. Martinko[a,1], Erin F. Simonds[a,1], Suchitra Prasad[a], Alberto Ponce[a,2], Colton J. Bracken[b], Junnian Wei[c], Yung-Hua Wang[c], Tiffany-Lynn Chow[a,3], Zhong Huang[a], Michael J. Evans[c], James A. Wells[d,e], and Zachary B. Hill[a,4]

[a]Department of Research and Development, Soteria Biotherapeutics, Inc., San Mateo, CA 94403; [b]Chemistry and Chemical Biology Graduate Program, University of California, San Francisco, CA 94107; [c]Department of Radiology and Biomedical Imaging, University of California, San Francisco, CA 94107; [d]Department of Pharmaceutical Chemistry, University of California, San Francisco, CA 94107; and [e]Department of Cellular and Molecular Pharmacology, University of California, San Francisco, CA 94107

Edited by Michael Oldstone, Department of Immunology and Microbiology, The Scripps Research Institute, La Jolla, CA; received October 13, 2021; accepted January 4, 2022

The antigen specificity and long serum half-life of monoclonal antibodies have made them a critical part of modern therapeutics. These properties have been coopted in a number of synthetic formats, such as antibody–drug conjugates, bispecific antibodies, or Fc-fusion proteins to generate novel biologic drug modalities. Historically, these new therapies have been generated by covalently linking multiple molecular moieties through chemical or genetic methods. This irreversible fusion of different components means that the function of the molecule is static, as determined by the structure. Here, we report the development of a technology for switchable assembly of functional antibody complexes using chemically induced dimerization domains. This approach enables control of the antibody's intended function in vivo by modulating the dose of a small molecule. We demonstrate this switchable assembly across three therapeutically relevant functionalities in vivo, including localization of a radionuclide-conjugated antibody to an antigen-positive tumor, extension of a cytokine's half-life, and activation of bispecific, T cell–engaging antibodies.

antibodies | chemical biology | biologics | chemically induced dimerization

Antibodies are multidomain proteins that have become an important therapeutic platform for a wide range of diseases (1). The key feature of antibodies that enables broad therapeutic application is their ability to couple selective molecular targeting to a functional output in a single molecule with long serum half-life. In the example of natural antibodies, targeting of pathogen-associated antigens is coupled to functions that facilitate an immune response, such as antibody-dependent cellular cytotoxicity via the recruitment of natural killer cells. In the case of antibody-based therapeutics, targeting of disease-specific antigens can be linked in a modular way to a myriad of desired natural or synthetic effector domains. These can include radionuclides, cytotoxic payloads, immune cell engagers, cytokines, and engineered cells (2–6).

Historically, genetic and chemical techniques have been used to generate synthetic combinations of multiple domains that collectively impart both targeting and function into a single therapeutic molecule. This is exemplified by the wide array of antibody and protein fusion formats with unique specificities and therapeutic mechanisms that have entered the clinic to date (3–5, 7, 8). Despite the diversity of formats, the functional properties of these synthetic proteins are intrinsically defined by their chemical structures (Fig. 1*A*). Thus, once an antibody-based drug is infused into a patient, the clinician relinquishes any control over its activity, potentially for a period of weeks. The long half-lives can make it challenging to manage toxicities or to rapidly adjust drug activity in response to efficacy or pharmacodynamic biomarkers.

Several classes of antibody-based drugs could benefit from a method of rapidly controlling drug activity and exposure. One such class is therapeutically active proteins that have been fused to the Fc-region of human IgG, which imparts a longer serum half-life (5, 8). The Fc fusion strategy has extended the half-lives of diverse proteins, including cytokine receptors (e.g., etanercept and aflibercept), hormones (e.g., dulaglutide), and cytokine mimetics (e.g., romiplostim) but at the risk of prolonging their potentially toxic activity for weeks after injection. Another class of antibody-based drugs, bispecific T cell–engaging antibodies (bsTCEs), can potently redirect the immune system to attack cancer cells but are also associated with unmanageable toxicities that have been observed in early clinical trials (4, 7, 9). First-generation bsTCEs had short half-lives (<5 h) that allowed for rapid termination of treatment in response to toxicities but necessitated the use of burdensome continuous infusion pumps. Extended half-life bsTCEs were explored as a way to achieve more convenient dosing, but physicians lack a mechanism to quickly terminate activity in response to adverse events. Thus, efforts to increase the half-life of this powerful modality must be

Significance

Reported here, we describe a molecular protein technology to enable switchable assembly of functional antibody complexes. This approach, which we call ligand-induced transient engagement (LITE), allows for control of an antibody's intended function in vivo through the dosing of a small-molecule activator. Chemical regulation of antibody therapeutics represents a treatment paradigm to provide physicians with precise control over the therapeutic activity of a biologic drug after it is administered to a patient. Ultimately, this approach may result in a new class of antibody drugs with improved efficacy and safety profiles and the potential to greatly impact the treatment of human disease.

Author contributions: A.J.M., E.F.S., M.J.E., J.A.W., and Z.B.H. designed research; A.J.M., E.F.S., S.P., A.P., C.J.B., J.W., Y.-H.W., T.-L.C., and Z.H. performed research; A.J.M., E.F.S., S.P., A.P., C.J.B., J.W., Y.-H.W., T.-L.C., Z.H., and M.J.E. analyzed data; and A.J.M., E.F.S., and Z.B.H. wrote the paper.

Competing interest statement: J.A.W., Z.B.H., E.F.S., and A.J.M. are inventors on intellectual property related to this work. J.A.W., Z.B.H., E.F.S., A.J.M., C.J.B., A.P., and S.P. own shares in Soteria Biotherapeutics, Inc., a company that owns intellectual property related to this work. Z.B.H., E.F.S., A.J.M., Z.H., and S.P. are employees of Soteria Biotherapeutics, Inc. Z.B.H. is a Director of Soteria Biotherapeutics, Inc.

This article is a PNAS Direct Submission.

[1]A.J.M. and E.F.S. contributed equally to this work.

[2]Present address: Department of Research and Development, ArsenalBio, South San Francisco, CA 94080.

[3]Present address: Department of Research and Development, Scorpion Therapeutics, South San Francisco, CA 94080.

[4]To whom correspondence may be addressed. Email: zach@soteriabiotx.com.

This article contains supporting information online at http://www.pnas.org/lookup/suppl/doi:10.1073/pnas.2117402119/-/DCSupplemental.

Published February 24, 2022.

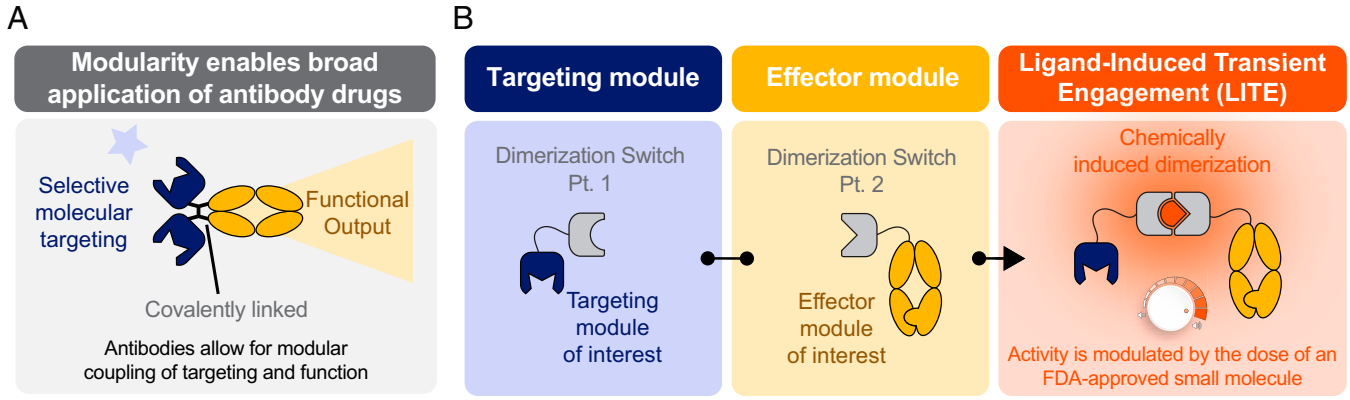

Fig. 1. LITE enables antibody complexes with switchable assembly and activity. (*A*) Most biologic drugs use a targeting domain to localize a functional, therapeutic moiety, but these molecular components are inextricably linked. (*B*) LITE is a technology to enable switchable assembly of individual antibody components into an active complex.

paired with approaches for managing toxicity. An ideal solution to address these challenges would combine the long half-life advantages of biologic drugs with the precise temporal control of activity associated with small molecules. An antibody-based drug with these features would allow for convenient dosing but also enable a clinician to quickly respond to a patient's needs by increasing drug activity or reversing toxicity.

Here, we demonstrate a general approach for ligand-induced transient engagement (LITE) of multiple antibody domains, whereby chemically induced dimerization is applied to enable switchable antibody activity by modulating the dose of an Food and Drug Administration (FDA)-approved small molecule (Fig. 1*B*). We provide three examples demonstrating the broad utility of this approach. First, we show the induced association of a tumor-targeting domain to reversibly control the biodistribution and tumor localization of an antibody in vivo. Second, we demonstrate that the inducible transient engagement of a therapeutically relevant cytokine to an Fc domain dramatically increases its half-life in vivo. Finally, we show small-molecule–regulated formation of a functional, bispecific T cell engager complex capable of redirecting T cells to kill tumor cells in vitro and in vivo. In summary, the LITE platform enables a new class of biologic drugs with functions that can be precisely switched on and off after intravenous (i.v.) administration.

Results

Generation of a Venetoclax-Inducible LITE Switch. Recently, we reported a method to rapidly generate antibody-based, chemically induced dimerizer (AbCID) systems based on existing small-molecule drugs (10). Conceptually, this approach can be applied to a large number of small molecules, but we sought to identify a clinically approved proof of concept molecule that could be applied to in vivo applications. With this in mind, we set out to build an AbCID that could be switched on by the orally available, small-molecule drug, venetoclax (formerly ABT-199, GDC-0199) (Fig. 2*A*). Venetoclax, a selective inhibitor of BCL-2, is clinically approved in the United States and Europe for the treatment of certain leukemias (11). Using an in vitro antibody–phage display selection approach with a naive Fab diversity library (10), we identified Fab fragments that selectively bound to the BCL-2/venetoclax complex over apo (venetoclax unbound) BCL-2 and did not bind venetoclax alone (*SI Appendix*, Figs. S1 and S2 and Table S1). From 26 unique clones, we identified AZ21, which displayed potent affinity ($K_D = 1.79 \times 10^{-9}$ M) and venetoclax-selective binding (Fig. 2 *B* and *C* and *SI Appendix*, Figs. S3 and S4 and Table S2). AZ21 showed exquisite chemoselectivity for venetoclax over the close structural analogs ABT-737 and navitoclax (Fig. 2*D*). This strongly supports that AZ21 recognizes a composite epitope that contains portions of venetoclax and BCL-2.

While the BCL-2/venetoclax/AZ21 complex showed small-molecule–dependent assembly, we sought a complex with rapid dissociation kinetics to enable reversible, switch-like behavior in vivo. However, the half-life of complex dissociation upon infinite dilution of venetoclax was ~4 d (*SI Appendix*, Fig. S5) with wild-type (WT) BCL-2. As venetoclax binds potently to BCL-2 with a K_i of <10 pM (12), we reasoned that dissociation of this interaction was the rate-limiting step for dissociation of AZ21/BCL-2 complex. Kinetic modeling of the system using a computational approach supported this hypothesis (*SI Appendix*, Fig. S6). We asked whether point mutations in the venetoclax binding site of BCL-2 could weaken its interaction with venetoclax and thereby reduce the half-life of the AbCID complex. Based on inspection of the crystal structure of the BCL-2/venetoclax complex (13), we identified three residues for mutagenesis (Fig. 2*E*) and measured the effects on the association and dissociation kinetics of the AbCID. As anticipated, several point mutations to BCL-2 decreased the half-life of the AbCID complex while maintaining similar association kinetics and affinities of AZ21 for the complex (Fig. 2*F* and *SI Appendix*, Fig. S7). The F103A mutation resulted in an AbCID with a 3.05-h half-life of complex dissociation. While the observed half-life of a switch complex for a given therapeutic application will be dependent on the concentrations, relative stoichiometries, and binding kinetics of the individual components, we selected the F103A mutant for proof-of-concept studies of reversible switch activity.

Armed with this toolbox of long-lived and rapidly reversible, venetoclax-based AbCIDs, we next turned our attention to the application of these molecular switches to control the association of antibody domains. We refer to this approach as LITE and as such will refer to the AbCID domains in this context as LITE Switches.

LITE Enables the Reversible Assembly and Tumor Localization of an Antibody Complex In Vivo. To initially investigate whether the LITE Switch could control the coupling of targeting and function in vivo, we designed an experiment to monitor venetoclax-induced recruitment of an antibody–radioligand bioconjugate to the site of an engrafted tumor. To enable real-time measurement of the biodistribution of the assembled complex in live mice, we turned to positron emission tomography (PET) and generated a switchable, bispecific system consisting of two antibody molecules. The first antibody contained an αCD19 single-chain variable fragment (scFv) and BCL-2 fused to a heterotypic knob/

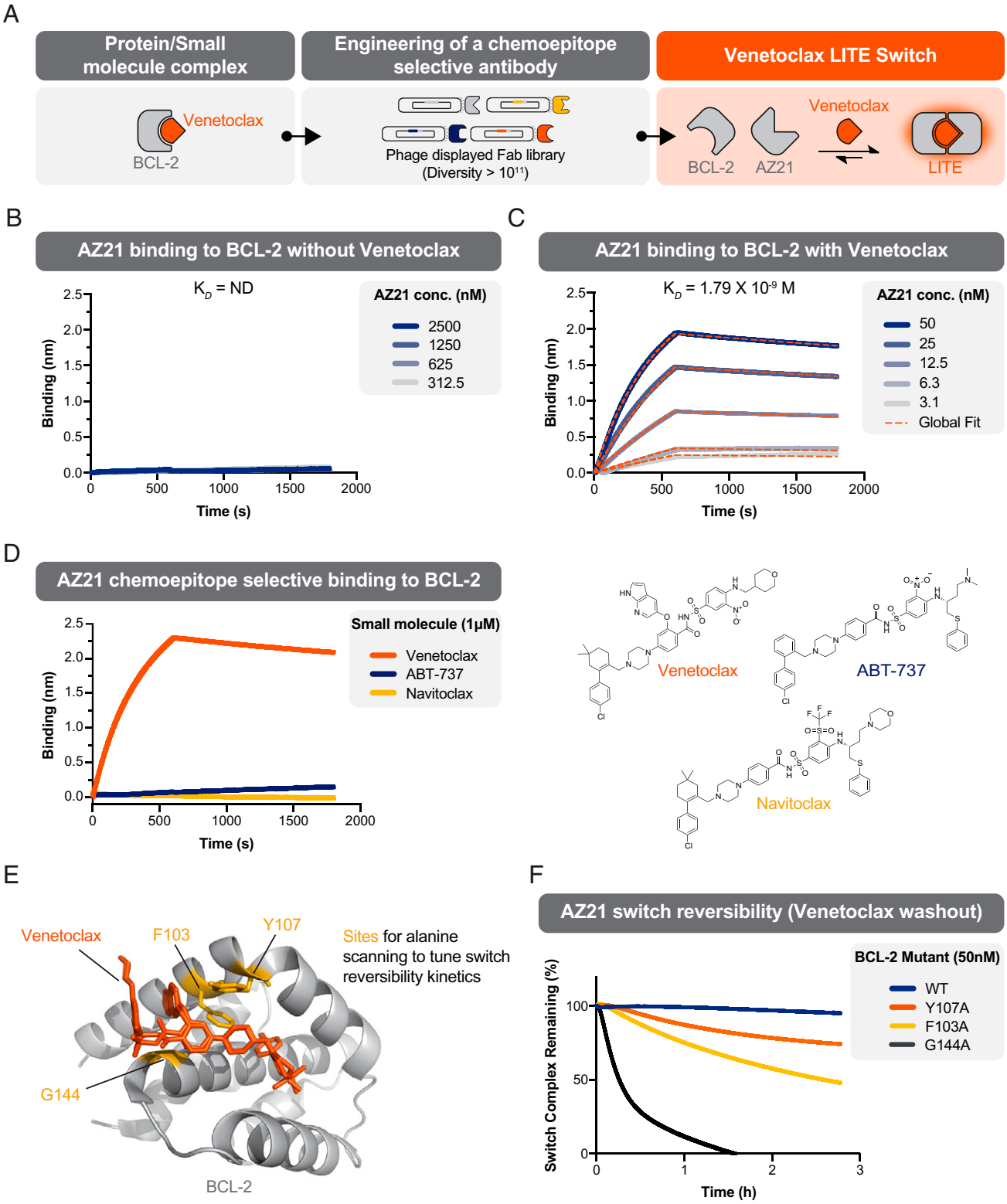

Fig. 2. Design and characterization of a reversible, venetoclax-dependent LITE Switch. (*A*) Schematic depicting the engineering of a venetoclax-inducible LITE Switch. (*B*) BLI shows no detectable binding (ND) of Fab AZ21 to BCL-2 in the absence of venetoclax. (*C*) BLI shows potent binding of Fab AZ21 to BCL-2 in the presence of 1 μM venetoclax. (*D*) BLI demonstrates that Fab AZ21 (50 nM) binds potently to BCL-2 in the presence of venetoclax but undetectably in the presence of chemical analogs ABT-737 or navitoclax. These data are consistent with the hypothesis that Fab AZ21 makes direct contacts with venetoclax when the latter is bound to BCL-2. (*E*) A crystal structure of BCL-2 in complex with venetoclax depicts sites that were chosen for rational mutagenesis to weaken the BCL-2/venetoclax interaction with the goal of increasing switch reversibility. (*F*) The kinetics of LITE Switch reversibility upon washout of venetoclax were measured by BLI. Data shows that the WT BCL-2 LITE Switch is practically irreversible on the timescale of hours. Mutant BCL-2 LITE Switches (G144A, F103A, and Y107A) showed markedly increased rates of dissociation upon venetoclax washout.

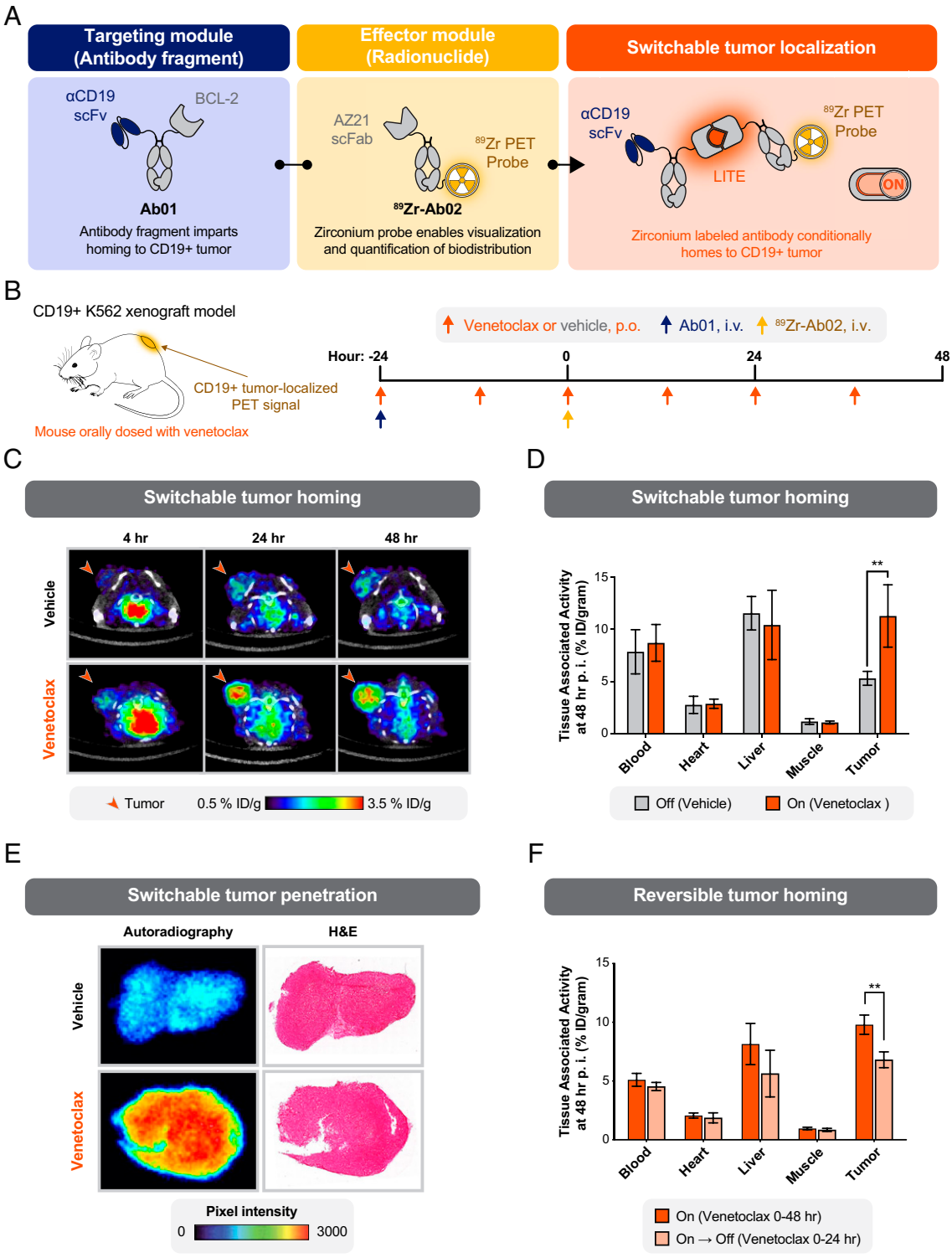

Fig. 3. Switchable localization of a radionuclide-conjugated antibody to a solid tumor. (*A*) Schematic of a protein design to enable switchable interaction between a CD19-targeting antibody fragment and an ^{89}Zr-labeled antibody for imaging by PET. (*B*) Study design to measure the biodistribution of the ^{89}Zr-labeled antibody. Antibodies were injected intravenously (i.v.) into immunocompromised mice bearing tumor xenografts engineered to overexpress human CD19. Venetoclax (10 mg/kg) or vehicle control was delivered by oral gavage (per os [p.o.]). (*C*) Representative transaxial PET/CT images showed venetoclax-dependent localization of PET signal to the tumor by 4-h postinjection (p.i.) and higher signal at 24 and 48 h. Minimal PET signal was detected in the tumors of mice treated with the oral gavage vehicle. Representative images from a single mouse per condition are shown. (*D*) Venetoclax treatment resulted in a significant increase in tumor-bound ^{89}Zr-Ab02 as quantified ex vivo (%ID/gram, percent injected dose per gram of tissue). No significant difference in ^{89}Zr-Ab02 uptake was observed between groups among normal tissues (error bars SEM; $n = 4$ per group; unpaired two-tailed t test; $^{**}P = 0.008$). (*E*) Autoradiography and hematoxylin and eosin (H&E) staining of representative tumor sections show the distribution of ^{89}Zr-Ab02 within tumors from mice treated with vehicle or venetoclax. ^{89}Zr-Ab02 penetrates the tumors of mice treated with venetoclax. Data presented are representative of four technical replicates. (*F*) Tumor binding of ^{89}Zr-Ab02 was significantly reversed when dosing of venetoclax was halted at 24 h after infusion of the antibodies. (error bars SEM; $n = 3$ to 4 per group; unpaired two-tailed t test; $^{**}P = 0.003$).

hole IgG Fc region (Ab01; Fig. 3*A*). This antibody was designed to bind to the engrafted tumor and to participate in the LITE Switch complex, but it intentionally lacked a positron-emitting radioisotope. The second antibody molecule contained an AZ21 single-chain Fab region (scFab) and was conjugated to ^{89}Zr for visualization with PET (^{89}Zr-Ab02; Fig. 3*A*). As ^{89}Zr-Ab02 lacks a tumor-targeting domain, we anticipated that it would distribute throughout the mouse without engaging in specific binding interactions. However, in the presence of venetoclax and formation of the LITE Switch complex, we hypothesized that ^{89}Zr-Ab02 would specifically bind to Ab01/CD19 in the tumor. To test this hypothesis, mice bearing subcutaneous, CD19-positive K562 tumors were given sequential i.v. injections of 1) Ab01 and 2) ^{89}Zr-Ab02 and administered either vehicle or venetoclax twice daily by oral gavage (Fig. 3*B*). The antibody injections were intentionally separated by 24 h to test if ^{89}Zr-Ab02 could engage the Ab01/CD19 complex after Ab01 had bound to CD19 in the tumor microenvironment. We avoided coinjection of Ab01 and ^{89}Zr-Ab02 because of the concern that the complex could form in the blood and preferentially biodistribute to the tumor because of its larger molecular weight, rather than specific targeting to CD19.

PET imaging showed a dramatic, time-dependent increase in tumor-localized emission in venetoclax-treated mice relative to the vehicle-treated mice, strongly supporting formation of the antibody complex at the tumor site. Tumor-localized radioactivity was evident 24 h after administration of ^{89}Zr-Ab02 and was further pronounced at 48 h. (Fig. 2*C*). At 48 h, tumors and organs from both groups of mice were harvested, and their level of radioactivity was quantified ex vivo. The venetoclax-treated group showed a statistically significant increase in PET signal in the tumor tissue but not in CD19-negative tissues. The absence of venetoclax-dependent accumulation in CD19-negative tissues underscores that the differential tumor uptake is likely driven by specific binding of the antibody complex to CD19, rather than nonspecific binding due to slower clearance of Ab01/venetoclax/^{89}Zr-Ab02 versus ^{89}Zr-Ab02 (Fig. 3*D* and *SI Appendix*, Fig. S8*A*).

To determine whether the assembled complex penetrated beyond the tumor surface, we performed autoradiography on tumor slices (*SI Appendix*, Fig. S9*A*). We observed robust radiolabel emissions from tumor cross-sections in venetoclax-treated mice, supporting that the three-component Ab01/venetoclax/^{89}Zr-Ab02 complex was capable of penetrating the tumor (Fig. 3*E*).

To demonstrate the reversibility of the LITE Switch in vivo, we performed a similar experiment to our initial PET study but used the rapidly reversible F103A mutant of BCL-2 (Ab01-rev). In this study, one group of mice was administered venetoclax for 48 h following injection of the antibodies ("On"), while in the other group venetoclax treatment was stopped after 24 h ("On → Off") (*SI Appendix*, Fig. S9*B*). Because venetoclax has a serum half-life of ∼2.7 h in mice (14), we anticipated a reduction in tumor-localized radioactivity at the 48-h time point in the mice that stopped receiving venetoclax. As predicted, the group that stopped receiving venetoclax after 24 h ("On → Off") showed significantly reduced emission at the tumor (Fig. 3*F*). These data support that the LITE Switch system enables temporal control over both the formation and dissociation of antibody complexes at specific sites in vivo.

The Plasma Half-life of an LITE Switch-Fused Therapeutic Protein Can Be Controlled Using a LITE Switch. The plasma half-life of a biologic therapeutic is a key pharmacokinetic property that often must be optimized during drug development. While antibodies generally exhibit long plasma half-lives due to Fc domain–mediated FcRn recycling, many therapeutically important proteins have very short natural half-lives, leading to a variety of half-life extension strategies to improve drug exposure and relieve the burden of frequent dosing (5). One such example of a rapidly cleared protein is interleukin-2 (IL-2). IL-2 is a critical cytokine that regulates lymphocyte proliferation and, paradoxically, the formation of immune tolerance. Because of its ability to stimulate an immune response, treatment with IL-2 was an early approach for cancer immunotherapy. High-dose IL-2 was approved for the treatment of melanoma and renal cell carcinoma, but it is notoriously difficult to dose effectively because of its very short serum half-life (∼6 min) (15) and severe side effects, which collectively result in a narrow therapeutic index (16). Fc fusions and chemical modifications of IL-2 (e.g., PEGylation) have been used to extend its half-life but at the risk of prolonging toxic side effects.

We wondered if the LITE Switch–mediated assembly of IL-2 into a complex containing an Fc domain would extend its plasma half-life, with the added benefit of being able to respond to toxic side effects by withdrawing the venetoclax dimerizer. To test this approach, we generated an AZ21-IL-2 fusion protein (Ab03) and the companion BCL-2-Fc fusion protein (Ab04) (Fig. 4*A*). Biophysical measurements showed that Ab03 retained the ability to bind BCL-2 in a venetoclax-dependent manner (Fig. 4 *B* and *C*). In cell-based assays, Ab03 stimulated the receptor (measured by phosphorylation of STAT5 on human T cells) with a similar potency as recombinant IL-2 (Fig. 4*D* and *SI Appendix*, Fig. S10). Together, these assays demonstrate that Ab03 maintained IL-2 functionality and a functional LITE Switch.

We next investigated if activating the LITE Switch would promote assembly of the Ab03/Ab04 complex in vivo and thereby extend the plasma half-life of Ab03. Mice were injected with a single i.v. dose of Ab03 (0.15 mg/kg) and Ab04 (5 mg/kg). Oral dosing with venetoclax (5 mg/kg) or vehicle began 2 h prior to the i.v. injection and was repeated daily. Plasma samples were collected from the mice at 3 min, 30 min, 1 h, 2 h, and 6 h after the i.v. injection. The concentration of Ab03 in the samples was measured by an enzyme-linked immunosorbent assay (ELISA) (Fig. 4*E*). As anticipated, Ab03 was rapidly cleared from the bloodstream (half-life: 8.6 min) in mice that received oral vehicle, exhibiting a half-life comparable to native IL-2 (15). However, in mice that received oral venetoclax, the half-life of Ab03 was extended by 17-fold (143.8 min: 2.4 h). This result indicates that LITE Switch–mediated association with Ab04 was capable of dramatically increasing the half-life of an otherwise short-lived biologic drug. Further work is needed to explore how this system could be employed in a therapeutic such that withdrawal of venetoclax results in accelerated clearance of the biologic drug. Specifically, if the elimination half-life of Ab03 could be extended much longer than the elimination half-life of venetoclax and the half-life of LITE Switch dissociation, then withdrawal of venetoclax would result in profoundly accelerated clearance of Ab03. Computational modeling supports that the half-life of Ab03 could be further increased through higher dosing of Ab04 (*SI Appendix*, Fig. S11).

LITE Enables the Formation of a bsTCE with Small-Molecule–Controlled Activity. Bispecific antibodies are molecules in which two different antibody paratopes, recognizing distinct targets, are combined in a single molecule. Bispecifics have become a prominent therapeutic paradigm, as exemplified by the >180 active programs in clinical development as of 2020 (17). In conventional bispecifics, the antibody paratopes are irreversibly linked, meaning the dual specificity of the molecule is hard-wired into its structure. In vitro noncovalent assembly of functional, T cell–engaging protein nanorings has previously been described, supporting that noncovalent, small-molecule–mediated interactions can maintain a functional immune synapse (18). However, assembly of these rings is based on a homodimeric assembly mechanism, necessitating their creation in vitro where stoichiometries of components can be tightly controlled to create a functional complex. In contrast, we

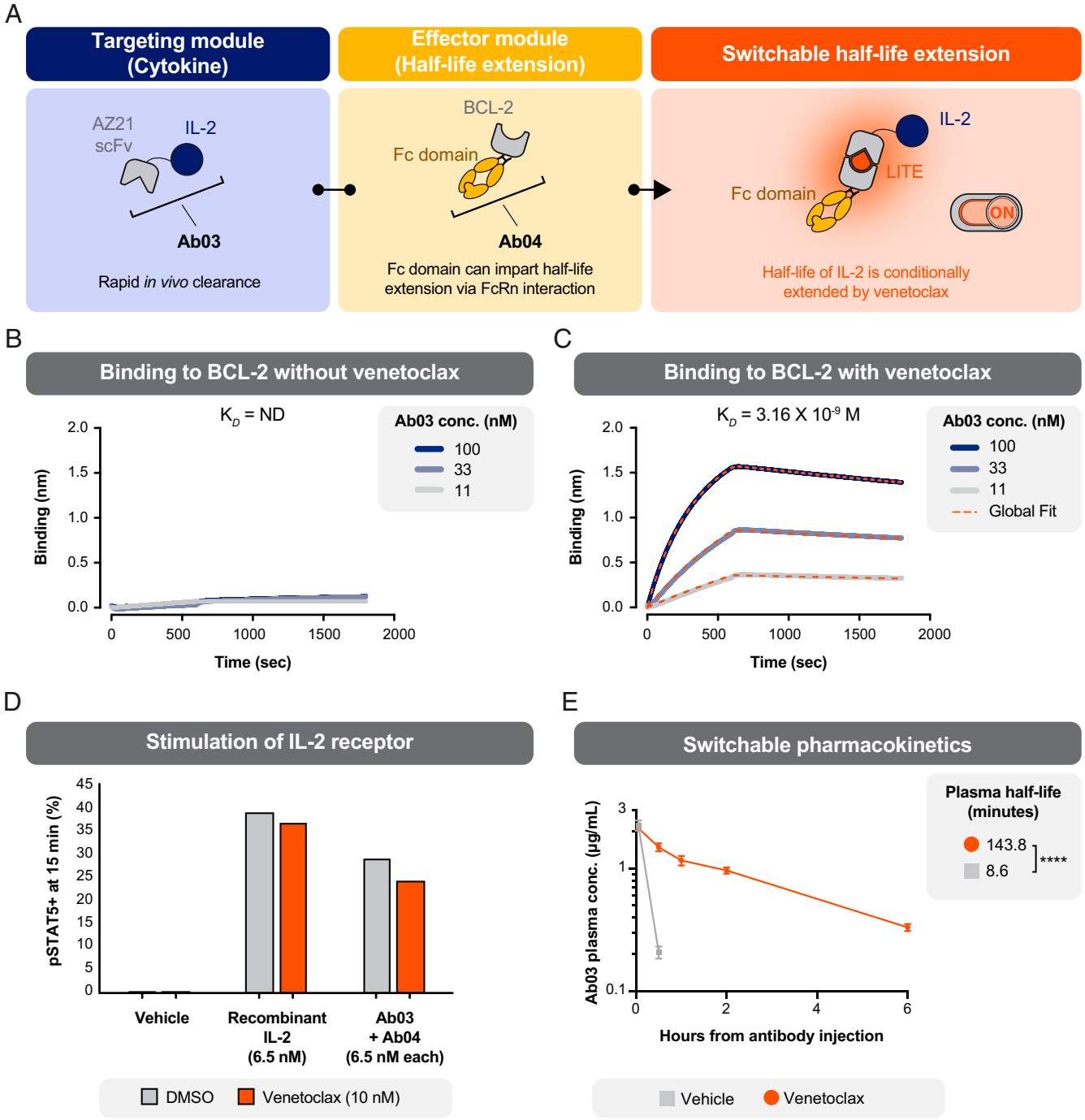

Fig. 4. The pharmacokinetic properties of a cytokine can be regulated through switchable association with an antibody Fc-domain. (*A*) Schematic of a protein design to enable switchable association of an antibody Fc-domain and the cytokine IL-2. (*B*) An AZ21-IL2 fusion (Ab03) exhibited no detectable binding (ND) to BCL-2 in the absence of venetoclax, as measured by BLI. (*C*) Ab03 showed potent binding to BCL-2 in the presence of venetoclax. (*D*) Ab03 was capable of driving signaling downstream of the IL-2 receptor, as indicated by phosphorylation of STAT5 in human T cells. Phospho-STAT5 was measured by intracellular flow cytometry after 15 min of treatment. The experiment was performed once without technical replicates. (*E*) The plasma clearance rate of Ab03 was slowed in mice that received Ab03, Ab04, and venetoclax. All mice were dosed intravenously at T = 0 h with Ab03 (0.15 mg/kg) and Ab04 (5 mg/kg). One group received venetoclax (5 mg/kg) by oral gavage (once daily starting at T = −2 h), and one group received vehicle control (error bars SEM; $n = 5$ per group; unpaired two-tailed t test ****$P < 0.0001$).

hypothesized that the LITE Switch could be applied to bring two antibody paratopes together in a transient and reversible complex, allowing temporal control over the functional activity. To explore this concept, we applied the LITE technology to create a switchable bsTCE (4, 7, 9). The clinical success of bsTCEs has been stymied by the potentially severe associated toxicities, so we reasoned that this class of drugs could benefit from the precise small-molecule control enabled by the LITE Switch technology.

We set about designing a two-antibody system in which a monovalent binder of the tumor-associated antigen (HER2) was fused to the BCL-2 half of the LITE Switch (Ab05), while a monovalent CD3-binding domain was fused to the AZ21 half

of the LITE Switch (Ab06). In this design, we envisioned that no T cell redirection or activation should occur in the absence of venetoclax. Upon addition of venetoclax, the Ab05/Ab06 complex should form a bridge between the two cells, resulting in activation of the T cell and killing of the HER2+ tumor cell (Fig. 5*A*). We refer to this system as T-LITE, for T cell LITE.

We cloned, expressed, and purified Ab05 and Ab06 and tested their function in coculture assays. Magnetically isolated, unactivated T cells from healthy donors were cocultured with HER2+ SKBR3 target cells. Both T-LITE antibodies were added at a constant concentration (10 nM) and the concentration of venetoclax was titrated. We observed venetoclax-dependent activation and redirection of T cells across multiple readouts: CD69 up-regulation, production of cytokines, and target cell killing (Fig. 5 *B* and *D* and *SI Appendix*, Fig. S12). The amount of venetoclax required for half-maximal target cell killing (EC_{50}) was 870 pM. To measure the potency of the T-LITE, we performed a similar coculture assay but titrated Ab06 in the presence or absence of venetoclax (10 nM) and constant Ab07 (10 nM). We observed T cell–dependent cellular cytotoxicity (TDCC) with an EC_{50} of 34 pM in the presence of venetoclax but minimal killing in the absence, thus further demonstrating the switchable activity of the T-LITE complex (*SI Appendix*, Fig. S13). We further profiled the kinetics of the coculture experiments using real-time fluorescent microscopy. The concentration of venetoclax affected the rate of target cell killing (e.g., the slope during hours 30 to 60 of coculture) (Fig. 5*E*). These kinetics suggest that the intermediate killing values, observed with concentrations of venetoclax near the EC_{50} in the 66 h coculture assay (Fig. 5*D*), were the result of slow but steady rates of infrequent killing events. This is consistent with the idea that a limiting amount of venetoclax maintains a small concentration of functional, bispecific complex at equilibrium.

To assess the reversibility of T cell activation and cytotoxic activity, we generated a T-LITE system incorporating the rapidly reversible F103A mutant of BCL-2 (Ab06-rev). Again, using real-time microscopy to follow the kinetics, we asked whether we could turn on and off target cell killing by changing the availability of venetoclax in the coculture system. To simulate the rapid metabolic clearance of venetoclax that would occur in an animal, we utilized purified BCL-2(WT) as a "molecular sponge." This molecule binds venetoclax with higher affinity than the F103A mutant, effectively sequestering venetoclax from the T-LITE antibodies and quenching their activity. Venetoclax or the molecular sponge were added in a variety of sequences, beginning 10 min after addition of the T-LITE antibodies. Consistent with previous experiments, constant activation of the T-LITE with venetoclax ("Always On") resulted in potent killing of the HER2+ SKBR3 cells, while the inactive complex ("Always Off") showed no cytolytic activity (Fig. 5*F*). Immediate quenching ("On → Off 30 m") resulted in a level of cytotoxicity comparable to Always Off, suggesting complete inactivation of the T-LITE. Quenching at 24 h ("On → Off 24 h") slowed the killing relative to the Always On condition, supporting that dissociation of the T-LITE complex, even at later time points in the assay, was capable of altering the extent of T cell cytotoxicity. Finally, we tested whether the system could be reactivated ("On → Off 30 m → On 24 h") by quenching immediately, then adding a fourfold excess of venetoclax 24 h later. Comparing this reactivated condition to the Always Off condition shows that despite 24 h of binding to the target cells in an inactive state, the T-LITE system could be reactivated to drive cell killing.

We next turned our attention to demonstrating T-LITE functionality in vivo. To this end, we characterized the efficacy of the T-LITE in a BT-474 admixed peripheral blood mononuclear cell (PBMC) xenograft model of HER2+ human breast cancer. In this model, venetoclax (or vehicle) administration by daily oral gavage was initiated on the day of randomization (Day 0), and a single dose of the HER2/CD3 T-LITE antibodies (Ab05 and Ab06) was administered (i.v.) on Day 1 (Fig. 5*G*). Consistent with the in vitro performance, the T-LITE caused transient regression and sustained growth inhibition of established tumors when venetoclax was coadministered, but tumor growth continued unabated in the absence of venetoclax (Fig. 5*H* and *SI Appendix*, Fig. S14). This result strongly supports the switch-like behavior of the T-LITE in vivo and demonstrates that the assembled T-LITE complex is efficacious in this model.

Taken together, these in vitro and in vivo results demonstrate that the LITE technology can be used to control the formation of a potent and reversible T-LITE complex, enabling the development of a new and improved class of temporally controlled, bispecific T cell engagers.

Discussion

We have demonstrated the use of our LITE platform to enable rapid, reversible, and tunable assembly of functional antibody complexes using a small-molecule dimerizer. We used this technology to control the tumor localization of a radioligand, the pharmacokinetic properties of a cytokine, and the antitumor activity of a bsTCE. These three examples demonstrate the flexibility of the LITE platform as a general strategy to regulate antibody activity on time scales much faster than the natural metabolic clearance of traditional biologic drugs.

Nearly all antibody-based therapeutics have long half-lives, allowing them to persist in a patient for weeks after a single infusion. While this can be desirable because it enables less frequent dosing, it can also extend the duration of side effects. This double-edged sword is particularly problematic for antibody drugs in which patient-to-patient variability is high or in which side effects are difficult to manage or life-threatening. The LITE approach may be broadly useful for engineering more precisely dosed and safer antibody therapeutics. In particular, we propose that LITE Switch–enabled bsTCEs—T-LITEs—may help overcome the adverse events reported in early clinical trials that have derailed otherwise promising therapies. Temporally controlled bsTCE drugs would enable facile step-up dosing and rapid reversibility of therapeutic activity. Both of these strategies are used clinically to mitigate toxicities of short-lived bsTCEs (19) but are difficult to achieve with conventional antibodies. Temporal control would also enable short-term, pulsatile dosing strategies that are impossible with conventional antibodies. Temporarily deactivating a bsTCE drug for a period of days could relieve chronic T cell stimulation and prevent T cell exhaustion, thereby improving the efficacy. This approach has shown promise preclinically with engineered T cell therapies (20, 21) and merits investigation with bsTCEs.

A LITE Switch–enabled antibody therapy requires at least three components (e.g., two antibodies and a small-molecule dimerizer), which increases the complexity of engineering and introduces new pharmacokinetic considerations. Complexity will also increase in terms of clinical development, in which careful considerations will be required to design a dosing paradigm to evaluate safety and efficacy. The tradeoff for this complexity is the power of temporal control and a new way to modulate therapeutic index. Therapeutic index of an antibody-based drug is often defined by its affinity for the target and its biodistribution, which are dictated by the earliest engineering decisions (e.g., valency, binding affinity, and isotype). The LITE Switch platform allows temporal control over therapeutic antibodies that is independent of these protein engineering constraints, allowing fine-tuning of antibody behavior in vivo. The pharmacokinetics of each component must be considered, but this is simplified partly by the sequential process of LITE Switch complex assembly. Since AZ21 does not bind to free

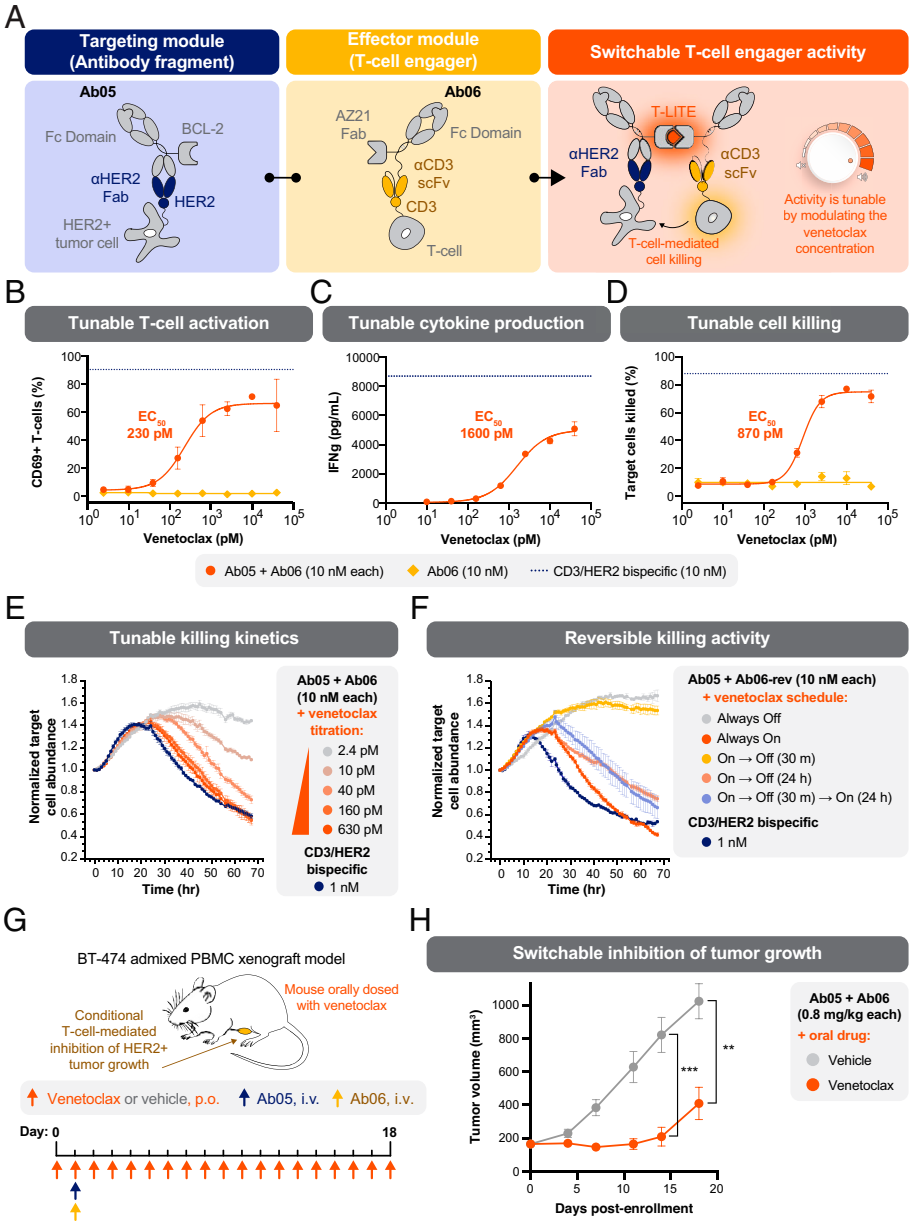

Fig. 5. Switchable T cell activation and redirected killing of HER2+ tumors with a bispecific T cell engager. (*A*) Schematic of a protein design to enable switchable assembly of a functional HER2/CD3 bispecific T cell engager. The redirection of T cells to kill target tumor cells can be tuned by modulating the concentration of venetoclax. (*B*) Activation of T cells in a coculture assay was dependent on the presence of venetoclax, as indicated by CD69 surface expression measured by flow cytometry. Primary human T cells were mixed with $HER2^+$ SKBR3 target cells at a ratio of 10:1 and treated with 10 nM of T-LITE antibodies (Ab05 and Ab06) at varying concentrations of venetoclax for 66 h. No activation was observed when only the anti-CD3 T-LITE Ab (Ab06) was added. Error bars SEM; $n = 3$ technical replicates. (*C*) Secretion of interferon gamma (IFNγ) by T cells in the coculture assay was chemically regulated by the concentration of venetoclax. Error bars SEM; $n = 3$ technical replicates. (*D*) TDCC of $HER2^+$ SKBR3 tumor cells is dependent on the concentration of venetoclax. Error bars SEM; $n = 3$ technical replicates. (*E*) The rate of TDCC, as assessed by time course microscopy, was dependent on the concentration of venetoclax. T cells (added at T = −2 h) and antibodies (added at T = −1 h) were present throughout the experiment; E:T ratio was 3:1. (*F*) The temporal flexibility of TDCC was explored using the rapidly reversible BCL-2 mutant F103A (Ab06-rev) and time-lapse microscopy. Different schedules of T cell activation were tested by changing the times when venetoclax (10 nM) was added to the coculture ("On") or sequestered by adding WT BCL-2 ("Off"). TDCC could be rapidly initiated (Always On), prevented (Always Off), and reversed ("On → Off"). Addition of more venetoclax (40 nM) caused reactivation of TDCC ("On → Off → On"). T cells (added at T = −2 h) and antibodies (added at T = −1 h) were present throughout the experiment; E:T ratio was 10:1. (*G*) Study design to evaluate switchable efficacy of an HER2-targeted T-LITE in an established xenograft tumor model. BT-474 breast cancer cells (8×10^6) were premixed with human PBMCs (8×10^6) and inoculated subcutaneously into the mammary fat pad of NCG mice on Day −9. Antibodies (0.8 mg/kg, each) were administered intravenously on Day 1, and venetoclax (5 mg/kg) was given by oral gavage (per os [p.o.]) daily beginning on Day 0. (*H*) In mice with established tumors (150 to 200 mm^3), a single dose of T-LITE antibodies (Day 1) caused tumor regression only when venetoclax was coadministered (Days 0 to 18). Error bars SEM; $n = 5$ per group; unpaired two-tailed *t* test; $^{**}P = 0.0010$ (Day 14); $^{***}P = 0.0038$ (Day 18).

venetoclax, there is no "hook effect" at high concentrations of venetoclax. This design simplifies the dosing of the small-molecule dimerizer, which can be administered at saturating levels without diminishing LITE Switch activation.

We chose venetoclax as the small-molecule dimerizer for this LITE Switch because it is an FDA-approved drug with a defined safety and pharmacokinetic profile in humans. We acknowledge that the underlying pharmacology of venetoclax

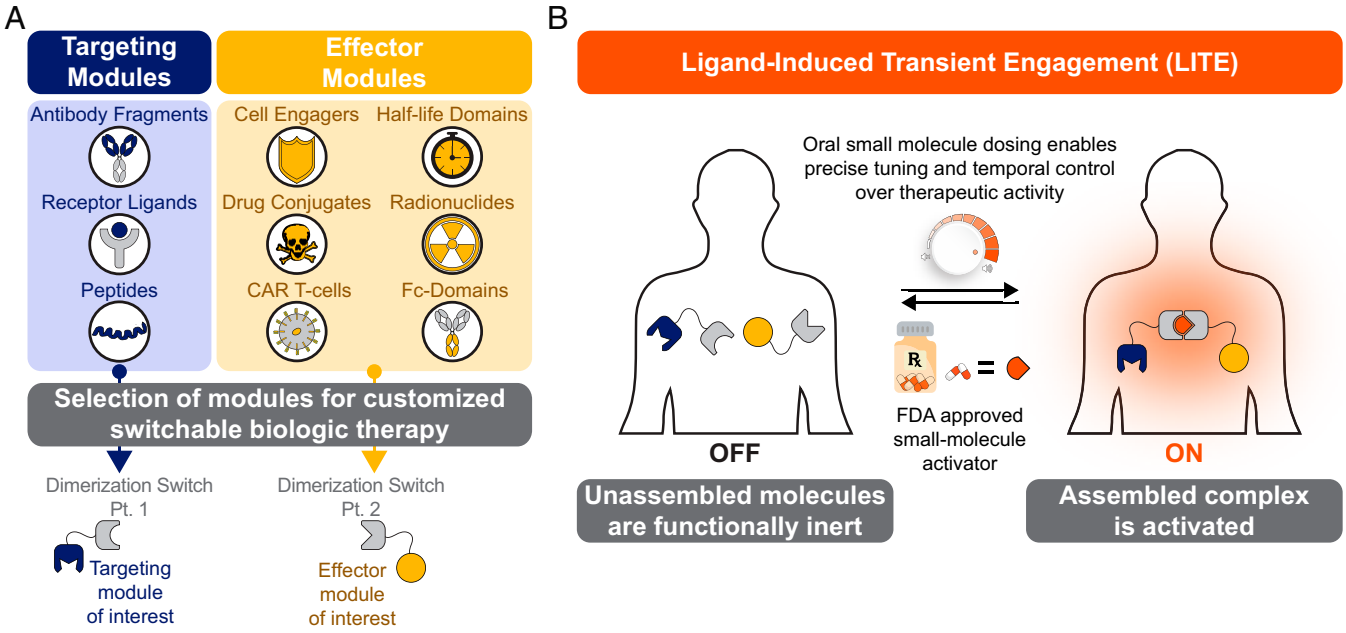

Fig. 6. A modular approach to engineering customized biologic drugs with chemically regulated activity. (*A*) Switchable biological therapies can be built through the selection of specific targeting and effector domains. (*B*) Under the paradigm of small-molecule–inducible biologic drugs, a patient would be dosed with the biologics, which would remain dormant and unassembled in the patient's serum. The patient can then take the orally available, small-molecule dimerizer drug, resulting in the rapid assembly of the LITE Switch and action of a functional biologic. This activity would be tunable via the dose and timing of the administration of the small molecule. Activity would be reversed through halted dosing of the small molecule.

may not be desirable for some therapeutic applications. Fortunately, the general nature of the LITE Switch approach allows for the rapid generation of CIDs using a variety of small molecules. The choice of small molecule could be customized for the desired application.

When thinking about constructing switchable biologics, there is the possibility that the switch components themselves could lead to unanticipated immunological effects. We deliberately built our LITE Switch entirely from human protein components to mitigate the risk of immunogenicity. However, the assembled complex may create novel epitopes at the interface of the LITE Switch components that elicit an immune response. While outside the scope of this manuscript, this possibility should be carefully studied as this technology advances.

Chemical regulation of antibody therapeutics has broad potential and represents a new paradigm for biologic drugs with remote control. Here, we have shown through several examples that this approach is easily adapted for customized pairing of targeting modules (e.g., antibodies, receptor ligands, peptides, etc.) and effector modules (e.g., immune cell engagers, drug conjugates, half-life extension domains, etc.) (Fig. 6*A*). This system could enable a physician to more precisely control the therapeutic activity of a biologic drug (Fig. 6*B*). The approach described here constitutes a conceptual path to integrate the diverse and potent activities of antibody-based therapeutics with the convenient dosing and pharmacokinetic timescales provided by orally available and rapidly metabolized small-molecule drugs.

Online Methods

Small-Molecule Reagents. Venetoclax-free base (>99%; LC Laboratories V-3579), ABT-737 (>99%; ChemieTek CT-A737), and ABT-263 (navitoclax) (>99%; Selleck Chemicals S1001) were obtained commercially and used without further purification.

Expression, Purification, and Biotinylation of BCL-2 and Mutants. BCL-2 (residues 2 to 207) in vector pMCSG7 was previously generated (10). Mutations Y107A, F103A, and G144A were introduced using site-directed mutagenesis. BCL-2 and mutants were expressed, purified, and biotinylated as previously described (10).

Antibody Expression and Purification. All antibodies were expressed and purified from Expi293F (Thermo Fisher Scientific) or modified Expi293 BirA-KDEL (22) cells, according to an established protocol from the manufacturer (Thermo Fisher Scientific). Culturing media for BirA cells was additionally supplemented with 100 μM biotin prior to transfection for in vivo biotinylation. Fc fusion proteins were purified by Protein A (MabSelect PrismA) affinity chromatography and His-tagged proteins were purified by Ni-NTA (Roche cOmplete His-Tag Resin) affinity chromatography. Eluted proteins from affinity purification were further separated by size-exclusion chromatography with a Superdex 200 increase 10/300 GL column (Cytiva) in storage buffer (1× Hepes buffered saline + 5% glycerol) as an aqueous phase. Purity and integrity were assessed by sodium dodecyl sulphate–polyacrylamide gel electrophoresis with 4 to 12% Bis-Tris precast gels (Thermo Fisher Scientific).

Phage Display Selections. Phage display selections were performed as previously described (10, 23, 24). Briefly, selections with antibody phage library F were performed using biotinylated BCL-2 captured with streptavidin-coated magnetic beads (Promega). Prior to each selection, the phage pool was incubated with 1 μM BCL-2 immobilized on streptavidin beads in the absence of venetoclax to deplete the library of any binders to the apo form of BCL-2. Subsequently, the beads were removed, and venetoclax was added to the phage pool at a concentration of 1 μM. In total, four rounds of selection were performed with decreasing amounts of BCL-2 antigen (100, 50, 10, and 10 nM).

Binding Kinetics Analysis. Biolayer interferometry (BLI) data were measured using an Octet RED384 (ForteBio) instrument. Biotinylated BCL-2 or BCL-2 mutants were immobilized on a streptavidin biosensor and loaded until a 0.4- to 0.6-nm signal

was achieved. After blocking with 10 μM biotin, 1 μM small molecule or 0.05% DMSO vehicle was loaded. Purified Fabs were used as the analyte premixed with 1 μM small molecule or 0.05% DMSO vehicle. During washout experiments, disassociation steps were performed in the absence of venetoclax and in the presence of 50 nM Fab. PBSTB (phosphate buffered saline [PBS], pH 7.4, 0.05% Tween-20, 0.2% bovine serum albumin [BSA]) was used for all buffers for BLI. Data were analyzed using ForteBio Octet analysis software, and kinetic parameters were determined using a 1:1 monovalent binding model. Unless otherwise noted, all BLI data presented were generated from an experiment performed once.

Small-Animal PET and Biodistribution Studies. All PET studies were conducted in compliance with the Institutional Animal Care and Use Committee at the University of California, San Francisco. A 3- to 5-wk-old male *nu/nu* were obtained from Charles River and were inoculated with 2×10^6 K562/CD19$^+$ cells subcutaneously in the flank as a 1:1 mixture volume percent (vol/vol) of base media and Matrigel (Corning). Tumors were palpable within 21 to 28 d after injection. Ab02 (8 μg) was diluted in 100 mL saline and injected into each mouse via tail vein injection at day −1. Then, the tumor-bearing mice were treated twice daily via oral gavage with 10 mg/kg venetoclax or vehicle.

Tumor-bearing mice ($n = 4$ to 5 per treatment arm) received ∼100 μCi of ^{89}Zr-Ab01 in 100 μL volume intravenously using a custom mouse tail vein catheter with a 28-gauge needle and a 100- to 150-mm long polyethylene microtubing (0.28 mm inside diameter, 0.64 mm outside diameter, Scientific Commodities, Inc.). For Ab01, after the injection, the mice were treated twice daily via oral gavage with 10 mg/kg venetoclax or vehicle. For the reversibility experiment, the rapidly reversible BCL-2 mutant F103A was used in Ab01 (Ab01-rev). One group of the mice were treated twice daily via oral gavage with 10 mg/kg venetoclax, while the other group were not treated with venetoclax after 24-h postinjection.

The mice were imaged on a dedicated small animal PET/CT scanner (Inveon, Siemens Healthcare) at the designed time points postinjection. Animals were scanned for 20 min for PET and 10 min for the computed tomography (CT) acquisition. The coregistration between PET and CT images was obtained using the rigid transformation matrix from the manufacturer-provided scanner calibration procedure, since the geometry between PET and CT remained constant for each of PET/CT scans using the combined PET/CT scanner. Animals were anesthetized with gas isoflurane at 2% concentration mixed with medical grade oxygen.

Manufacturer-provided, ordered subsets expectation maximization algorithm was used for PET reconstruction that resulted in 128'128'159 matrices with a voxel size of 0.776 × 0.776 × 0.796 mm^3. The CT image was created using a conebeam Feldkamp reconstruction algorithm (COBRA) provided by Exxim Computing Corporation. The matrix size of the reconstructed CT images was 512'512'662 with an isotropic voxel size of 0.191'0.191'0.191 mm^3. The photon attenuation correction was performed for PET reconstruction using the coregistered, CT-based attenuation map to ensure the quantitative accuracy of the reconstructed PET data.

To evaluate the uptake of ^{89}Zr-C4 in the xenografts, biodistribution studies were conducted following imaging. Tissues were weighed and counted on a γ-counter for accumulation of ^{89}Zr radioactivity. A total of 0.5 μCi ^{89}Zr dissolved in 1 mL of water was used as the reference standard to calculate the microcurie. The mass of ^{89}Zr-mAb formulation injected into each animal was then measured and used to determine the total number of counts per minute by comparison to the reference vials. The data were background- and decay corrected, and the tissue uptake was expressed in units of percentage injected dose per gram of dry tissue.

Autoradiography. For the tumor penetration study, the representative tumors of the venetoclax group and vehicle group were collected and sliced into 20 μm thickness. The signals were collected by the superresolution storage phosphor screen (BAS-IP SR 2025E) for overnight exposure. And the film was read by the Amersham Typhoon phosphor imager at a resolution of 50 μm.

Measurement of Ab03 Pharmacokinetics in Mice. Mouse pharmacokinetics experiments were performed at The Jackson Laboratory under Institutional Animal Care and Use Committee (IACUC) protocol AUS 15006. The 7-wk-old C56BL/6J male mice were distributed to two groups ($n = 5$ per group). Ab03 and Ab04 were premixed in sterile PBS and injected intravenously at 0.15 (Ab03) and 5 mg/kg (Ab04), respectively. An oral formulation of venetoclax (1 mg/mL final) was prepared by sequentially adding DMSO (2.5% final vol/vol), ethanol (10% final vol/vol), Cremophor EL (Miltenyi Biotec) (20% final vol/vol), and 5% dextrose water (67.5% final vol/vol). Oral formulations of venetoclax or vehicle control were administered at 5 mg/kg by oral gavage at seven time points (−2 d, 22 h, 46 h, 70 h, 94 h, 142 h, and 166 h). Blood (25 μL from retroorbital sinus) was sampled serially at nine time points (−14 d, 3 min, 30 min, 1 h, 2 h, 6 h, 24 h, 48 h, 72 h, and 168 h), processed to plasma, diluted 1:10 in 50% glycerol + PBS, and then cryopreserved. Plasma concentrations of Ab03 were quantified by human IL-2 Quantikine ELISA (R&D Systems) according to the manufacturer's instructions. Plasma concentrations of Ab04 were quantified using the human IgG ELISA BASIC kit (ALP) (Mabtech AB) according to the manufacturer's instructions. Noncompartmental pharmacokinetic parameters were calculated using PK Solutions software (Summit Research Services).

In Vitro Measurement of T Cell Activation, Cytokine Production, and Cytotoxicity. Coculture assays were used to assess T cell activation (CD69 up-regulation), cytokine production, or TDCC of SK-BR-3 target cells. Flat-bottom 96-well plates were seeded with 5,000 target cells in complete growth media (Dulbecco's modified Eagle medium + 10% fetal bovine serum + 1% penicillin/streptomycin) 16 to 24 h before the assay. Growth media was removed, and target cells were labeled with carboxyfluorescein diacetate succinimidyl ester (CFSE) in PBS (1.5 μM final concentration, 10 min at 37 °C) (Tonbo Biosciences). PBS was removed and replaced with 50 μL complete growth media. Magnetically isolated human T cells were thawed, washed, and resuspended in complete growth media, then added to target cells (50,000 T cells per well in 30 μL growth media). The final effector:target (E:T) ratio was 10:1. Biologic drugs (e.g., Ab05, Ab06, or CD3 × HER2 bispecific) were added in 10 μL growth media and incubated for at least 10 min at 37 °C. Venetoclax or vehicle control was added in 10 μL growth media for a final assay well volume of 100 μL. Assay plates were incubated at 37 °C with 5% CO_2 for 66 to 70 h, depending on the experiment. Culture media and T cells were transferred to a U-bottom 96-well plate and spun (400 rcf × 5 min). Supernatants were stored at −20 °C for later analysis of cytokines. T cells were resuspended in CF405M viability dye (0.5 μM, Biotium) in PBS for 10 min at 37 °C. Target cells were incubated with CF405M viability dye (0.5 μM, Biotium) diluted in TrypLE Express (Thermo Fisher Scientific) for 10 min at 37 °C. At the end of viability staining, cells were fixed by adding methanol-free paraformaldehyde (Electron Microscopy Sciences) to a final concentration of 1% for 10 min at room temperature. Dissociated target cells were transferred to the U-bottom 96-well plates containing T cells then spun (600 rcf × 5 min). Fixed cells were

resuspended in PE-conjugated anti-human CD69 (BioLegend) at a 1:16 final dilution and stained 30 min at room temperature before acquisition on an IntelliCyt iQue3 flow cytometer (Sartorius AG). Target cells killed (percentage) were calculated as the percentage of CF405M-positive events within the CFSE-positive population. CD69+ T cells (percentage) were calculated as the percentage of CD69-positive events within the CFSE-negative, CF405M-negative population. Dose–response curves and EC_{50} values were calculated in GraphPad Prism 9 software (GraphPad Software). Cytokine production was measured using the LEGENDplex human Th1 panel (5-plex) (BioLegend) according to the manufacturer's instructions and data acquisition on the iQue3 cytometer.

Real-Time Measurement of Target Cell Killing by Time-Lapse Microscopy. Cocultures of magnetically isolated human T cells and SK-BR-3 target cells were prepared as described in *In Vitro Measurement of T Cell Activation, Cytokine Production, and Cytotoxicity*, with some modifications. Prior to seeding, target cells were labeled with CellTracker Red CPTMX (1.57 μM final concentration, 30 min at 37 °C) (Thermo Fisher Scientific), then washed once with complete growth media. CFSE staining was not performed. Cocultures with appropriately diluted drugs were set up in flat-bottom 96-well plates in 150 μL final volume. E:T ratios were either 3:1 or 10:1, as indicated in the figures. Plates were imaged on an IncuCyte S3 live-cell analysis system (Sartorius AG) once per hour starting when venetoclax (10 nM final concentration) was added. In some wells, a molecular sponge (WT BCL-2 fused to a human heterodimeric Fc domain; 20 nM final concentration) was added to sequester-free venetoclax. In some wells, additional venetoclax (40 nM final concentration) was added to reactivate the T-LITE. The molecular sponge, additional venetoclax, or an equivalent volume of control media was added at the time points indicated in the figures. The IncuCyte software was used to quantify normalized target cell abundance (red object area per image, normalized to T = 0 h).

Measurement of T-LITE Efficacy in a BT-474 Adoptive Transfer Mouse Xenograft Model. Mouse efficacy experiments were performed at Crown Bioscience (Taicang). Any procedures involving the care and use of animals were reviewed and approved by the IACUC of CrownBio prior to execution and conducted in accordance with the regulations of the Association for Assessment and Accreditation of Laboratory Animal Care. The 10-wk-old NOD severe combined immunodeficiency gamma (NCG) female mice (Jiangsu GemPharmatech) were distributed to six groups ($n = 5$ per group). Mice were implanted with one 0.36-mg estradiol pellet in the right flank on Day −10. On Day −9, they were inoculated in the right mammary fat pad with 8 million tumor cells premixed with 8 million nonactivated, freshly isolated human PBMCs in 200 μL PBS + 50% Matrigel (Corning Life Sciences). Mice were measured twice weekly for body weight and tumor volume and randomized according to tumor volumes on Day 0 (when groups reached 150 to 200 mm^3 mean tumor volume). T-LITE antibodies (0.8 mg/kg Ab05 + 0.8 mg/kg Ab06) or conventional HER2 × CD3 bispecific (1 mg/kg) were administered intravenously on Day 1. Venetoclax oral solution (or vehicle control) was formulated as described in *Measurement of Ab03 Pharmacokinetics in Mice* and administered by oral gavage once daily beginning on Day 0. Statistical tests to compare tumor volumes (unpaired two-tailed *t* test) were performed in GraphPad Prism 9 software (GraphPad Software).

Thermodynamic Modeling. All thermodynamic modeling was performed with R in Rstudio utilizing the previously published deSolve package with the equations described in *SI Appendix*, Figs. S6*A* and S11*A*. All code is freely available on GitHub at https://github.com/alexmartinko.

Extended methods can be found in *SI Appendix*.

Data Availability. Code has been deposited in GitHub (https://github.com/alexmartinko). All other study data are included in the article and/or *SI Appendix*.

ACKNOWLEDGMENTS. We thank Meghan Zubradt for productive conversations related to Fc dimer–mediated half-life extension and for oversight of research timelines. We thank Megan Moore for her efforts during her rotation in the Wells laboratory. We thank Joe Lobel for his help with kinetic modeling. We thank Victoria Assimon for useful input on figure aesthetics. Portions of research reported in this publication was supported by the National Cancer Institute of the NIH under Award Number R43CA240063. The content is solely the responsibility of the authors and does not necessarily represent the official views of the NIH. J.A.W. acknowledges funding from NIH NCI CA191018, NIH GM097316, NIH R35GM122451, and the Harry and Dianna Hind Professorship.

1. R.-M. Lu *et al.*, Development of therapeutic antibodies for the treatment of diseases. *J. Biomed. Sci.* **27**, 1 (2020).
2. G. Sgouros, L. Bodei, M. R. McDevitt, J. R. Nedrow, Radiopharmaceutical therapy in cancer: Clinical advances and challenges. *Nat. Rev. Drug Discov.* **19**, 589–608 (2020). Correction in: *Nat. Rev. Drug Discov.* **19**, 819 (2020).
3. P. Khongorzul, C. J. Ling, F. U. Khan, A. U. Ihsan, J. Zhang, Antibody-drug conjugates: A comprehensive review. *Mol. Cancer Res.* **18**, 3–19 (2020).
4. A. F. Labrijn, M. L. Janmaat, J. M. Reichert, P. W. H. I. Parren, Bispecific antibodies: A mechanistic review of the pipeline. *Nat. Rev. Drug Discov.* **18**, 585–608 (2019).
5. W. R. Strohl, Fusion proteins for half-life extension of biologics as a strategy to make biobetters. *BioDrugs* **29**, 215–239 (2015).
6. S. Feins, W. Kong, E. F. Williams, M. C. Milone, J. A. Fraietta, An introduction to chimeric antigen receptor (CAR) T-cell immunotherapy for human cancer. *Am. J. Hematol.* **94** (S1), S3–S9 (2019).
7. F. V. Suurs, M. N. Lub-de Hooge, E. G. E. de Vries, D. J. A. de Groot, A review of bispecific antibodies and antibody constructs in oncology and clinical challenges. *Pharmacol. Ther.* **201**, 103–119 (2019).
8. R. Jafari, N. M. Zolbanin, H. Rafatpanah, J. Majidi, T. Kazemi, Fc-fusion proteins in therapy: An updated view. *Curr. Med. Chem.* **24**, 1228–1237 (2017).
9. O. Vafa, N. D. Trinklein, Perspective: Designing T-cell engagers with better therapeutic windows. *Front. Oncol.* **10**, 446 (2020).
10. Z. B. Hill, A. J. Martinko, D. P. Nguyen, J. A. Wells, Human antibody-based chemically induced dimerizers for cell therapeutic applications. *Nat. Chem. Biol.* **14**, 112–117 (2018).
11. I. Kapoor, J. Bodo, B. T. Hill, E. D. Hsi, A. Almasan, Targeting BCL-2 in B-cell malignancies and overcoming therapeutic resistance. *Cell Death Dis.* **11**, 941 (2020).
12. A. J. Souers *et al.*, ABT-199, a potent and selective BCL-2 inhibitor, achieves antitumor activity while sparing platelets. *Nat. Med.* **19**, 202–208 (2013).
13. R. W. Birkinshaw *et al.*, Structures of BCL-2 in complex with venetoclax reveal the molecular basis of resistance mutations. *Nat. Commun.* **10**, 2385 (2019).
14. Food and Drug Administration, "Pharmacology/toxicology NDA review and evaluation" (Tech. Rep. NDA 208573, 2015). https://www.accessdata.fda.gov/drugsatfda_docs/nda/2016/208573Orig1s000PharmR.pdf. Accessed 17 February 2022).
15. M. T. Lotze, R. J. Robb, S. O. Sharrow, L. W. Frana, S. A. Rosenberg, Systemic administration of interleukin-2 in humans. *J. Biol. Response Mod.* **3**, 475–482 (1984).
16. A. Tang, F. Harding, The challenges and molecular approaches surrounding interleukin-2-based therapeutics in cancer. *Cytokine X* **1**, 100001 (2019).
17. Beacon Targeted Therapies, Data from "Beacon Bispecific Database". https://beacon-intelligence.com/solutions/bispecific/. Accessed 17 February 2022.
18. J. R. Petersburg *et al.*, Eradication of established tumors by chemically self-assembled nanoring labeled T cells. *ACS Nano* **12**, 6563–6576 (2018).
19. M.-E. Goebeler *et al.*, Bispecific T-cell engager (BiTE) antibody construct blinatumomab for the treatment of patients with relapsed/refractory non-hodgkin lymphoma: Final results from a phase I study. *J. Clin. Oncol.* **34**, 1104–1111 (2016).
20. E. W. Weber *et al.*, Transient rest restores functionality in exhausted CAR-T cells through epigenetic remodeling. *Science* **372**, eaba1786 (2021).
21. S. Viaud *et al.*, Switchable control over in vivo CAR T expansion, B cell depletion, and induction of memory. *Proc. Natl. Acad. Sci. U.S.A.* **115**, E10898–E10906 (2018).
22. A. J. Martinko *et al.*, Targeting RAS-driven human cancer cells with antibodies to upregulated and essential cell-surface proteins. *eLife* **7**, e31098 (2018).
23. M. Hornsby *et al.*, A high through-put platform for recombinant antibodies to folded proteins. *Mol. Cell. Proteomics* **14**, 2833–2847 (2015).
24. A. J. Martinko, "Development of antibody tools to interrogate and modulate cellular signaling in cancer," PhD thesis, University of California, San Francisco, CA (2018).

BIOCHEMISTRY